Check for updates

Comparative analysis of metal contaminants and environmentally persistent free radicals in indoor dust from urban and rural households

Emily R. Halpern, [ID] [a] Steven Sharpe, [ID] [a] Killian MacFeely,[a] Peter Christ,[a] Lauren Heirty,[a] Christopher P. West, [ID] [a] Tuong Van Nguyen,[a] Satya S. Patra,[c] Brian H. Magnuson, [ID] [c] Brandon E. Boor,[c] Paige A. Thompson,[d] Laura J. Claxton,[d] Orit Herzberg,[e] Meghan Kalvey,[e] Margaret Shilling,[e] Karen E. Adolph[e] and Alexander Laskin [ID] *[ab]

Indoor dust is recognized as a reservoir of chemical toxicants owing to its high surface area and propensity for contact transfer and resuspension. It is an indicator of indoor pollutants and a potential source for exposure from ingestion and inhalation. To identify health-risks, house dust samples collected from urban (New York City, NY) and rural (West Lafayette, IN) residences were analyzed for two toxicant classes – toxic metals and environmentally persistent free radicals (EPFRs). Elemental composition and concentrations were quantified by X-ray fluorescence (XRF) spectroscopy and inductively coupled plasma-mass spectrometry (ICP-MS). Higher levels of crustal mineral elements (Na, Al, Si, Mg, P, S, Cl, K, Ca, Ti, Fe, and Mn) were observed in the rural dust samples (typically 2−5× higher in concentration), whereas several toxic metals were concentrated in the urban dust samples (Zn ≈ 430 ppm_m, Pb ≈ 100 ppm_m, Cu ≈ 70 ppm_m), corresponding to 2−3× higher concentrations. Analysis of elemental enrichment factors (EFs) indicated enhancement of several industrially relevant metals. Geospatial autocorrelation using Moran's Index revealed significant spatial clustering of several toxicologically relevant elements in the rural area, whereas most toxic elements in the urban area were randomly distributed, consistent with distinct source profiles. EPFR type and abundance were evaluated by electron paramagnetic resonance spectroscopy. Despite overlapping signals, several source-consistent components were identified through comparison with previous studies. The EPFR concentrations in these house dust samples spanned a wide range of 10^9–10^{16} radicals μg^{-1} dust. This systematic screening framework enables source apportionment of indoor dust contaminants and supports evaluation of potential health impacts.

Environmental significance

Indoor dust is a chemically active reservoir and vector of toxicants, including heavy metals and environmentally persistent free radicals, that accumulate from indoor and outdoor sources. These contaminants can re-enter the air or transfer to surfaces *via* contact pathways, contributing to exposure *via* inhalation, ingestion, and dermal uptake. This study demonstrates a systematic methodology to identify and quantify these toxicants in house dust from two regions in the United States. Additionally, it presents methods to assist source apportionment of these toxicants and identification of species of concern.

Introduction

As time spent indoors increases, the complex chemistry of indoor environments and associated hazards warrants closer examination. Indoor chemistry is shaped by mixing indoor emissions with infiltrating outdoor pollutants; it is multifaceted and remains incompletely characterized. The indoor environment is largely regulated by occupant behavior, preferences, and activities, whereas infiltration of outdoor pollutants varies with season, land use, and geographic location.[1] Indoor dust and the associated pollutants are also exposed to different conditions of temperature, humidity, and light exposure regulated by human activity. Reduced air exchange and surface-rich micro environments often yield higher pollutant concentrations and longer residence times indoors than outdoors.[2] Despite the potential for exposure, many indoor chemical hazards remain insufficiently characterized and unregulated, underscoring the

[a]Department of Chemistry, Purdue University, West Lafayette, IN, USA. E-mail: alaskin@purdue.edu

[b]Department of Earth, Atmospheric, and Planetary Sciences, Purdue University, West Lafayette, IN, USA

[c]Lyles School of Civil and Construction Engineering, Purdue University, West Lafayette, IN, USA

[d]Department of Health and Kinesiology, Purdue University, West Lafayette, IN, USA

[e]Department of Psychology, New York University, New York City, NY, USA

need for efficient screening approaches to access toxicants and advance understanding of indoor multiphase chemistry.[1]

Comprehensive evaluation is confounded by transient partitioning of species among the gas phase, particulate matter, and surfaces. Indoor dust has been of particular interest in recent years because it serves as a long-lived reservoir and carrier of toxicants within residences.[3] Toxicants from indoor dust can reach occupants through ingestion, inhalation of resuspended particles, and dermal contact.[4] Infants and toddlers face elevated risk because of frequent hand-to-mouth activities and proximity to floors.[5,6] The large surface area of dust promotes gas–particle and gas–surface partitioning of chemicals between the gas and condensed phases, and supports aqueous microfilms that facilitate heterogeneous reactions.[1,3] Ambient particles deposit onto surfaces and accumulate in dust, which can be resuspended by occupant activity, amplifying indoor mixing and exposure.[7] Accordingly, chemical characterization of house dust provides an integrative measure of indoor chemistry and a means to identify potential toxicants. Toxic metals are of substantial concern in house dust owing to their persistence, high toxicity, and bioaccumulation potential.[2] Their health effects are diverse at elevated exposures.[8] Arsenic is both toxic and carcinogenic. Cadmium is highly toxic and carcinogenic, and tends to accumulate in plants due to efficient soil-to-plant transfer. Chromium hazard depends on its oxidation state: Cr(VI) is highly toxic and cancerogenic, while Cr(III) is substantially less hazardous. Iron is essential metal for life but can be toxic to humans at elevated exposures.[9] Copper and Nickel are both industrial source metals that are toxic but not classified as carcinogenic.[10] Lead is strongly neurotoxic and carcinogenic. In house dust (particularly from old paint), Pb exhibits high bioavailability.[9,11] Indoor burdens arise from both indoor sources (*e.g.*, paints, coatings, building materials) and outdoor-to-indoor transfer through soil and particulate matter,[12] with regional influences, such as industrial emissions, local burning, and on-road pollution often determining metal profiles.[13] Given the toxicity and wide range of sources, comprehensive elemental analysis of dust is essential for hazard evaluation and source attribution.

Environmentally persistent free radicals (EPFRs) are an emerging pollutant class frequently associated with particulate matter. Unlike most radicals, EPFRs can persist for days to years, resulting in high impact on chemical reactions and toxicological relevance.[14] They are common components of particulate matter emissions from tobacco smoke,[15] electronic cigarettes,[16] and incomplete combustion (*e.g.*, cooking, outdoor industrial processes, wildfires).[17] Complexation with metal centers can stabilize EPFRs, extending their lifetime.[17] Accordingly, metal-rich dust (notably containing Zn, Al, and Ti) may promote the persistence of EPFRs.[18,19] In indoor dust, EPFRs occur in soot, mineral/soil, and other particulate matrices.[20] Upon ingestion or inhalation, EPFRs can produce reactive oxygen species (ROS) *in vivo*,[17] contributing to oxidative stress and increased risks of cardiovascular and respiratory diseases under chronic exposure.[21] EPFRs also drive indoor chemistry by generating ROS in dust with water condensed on it.[3] Improved characterization of EPFRs sources, types, and abundances in

house dust is therefore critical to access their roles in indoor chemistry and exposure.

House dust is understudied as a source of human, and especially infants, health risks. Infants are uniquely vulnerable to indoor dust, an abundant reservoir of metals, organics, and microbes, because they mouth objects, crawl near floors, and inhale resuspended particles, yet current assessments lack a mechanistic link between behavior, dust properties, and exposure. Comprehensive characterization is challenging due to its complex composition and source apportionment. Here, a targeted framework is presented to identify major contributors to dust toxicity and to inform assessments of health impacts from indoor dust ingestion by infants. Chemical differences were determined between dust collected in West Lafayette, IN, and New York City, NY. Toxic metals and EPFRs were quantified as practical indicators of dust toxicity and composition, enabling rapid screening of indoor hazards. *K*-means clustering (a machine-learning method) was applied to identify compositionally similar dust samples and to evaluate seasonal changes in composition. Moran's Index (a geospatial clustering metric) was used to identify elements occurring at elevated concentrations in specific subregions of the urban and rural areas.[22] These complementary analytical and statistical approaches establish a standardized, comprehensive framework for evaluating dust toxicity and probing regional and socioeconomic influences on indoor chemical hazards.

Experimental methods

Dust collection

Dust samples were collected from households in West Lafayette (WL), IN (and the surrounding communities), and New York City (NYC), NY, as part of a broader effort investigating infant exposure to ingested dust. All participants' homes housed a family with an infant (3–24 months old). From summer 2022 through spring 2024, vacuum sampling targeted three locations per residence: entryway ($n = 9$), living/common room ($n = 66$), and infant bedroom ($n = 51$). The vacuumed area was standardized by flooring type: 0.25 m^2 on carpeted surfaces and 0.50 m^2 on non-carpeted surfaces to accommodate lower dust loading on hard floors. The indoor dust collection protocol is described in detail in our prior work.[23]

The individual dust samples were sieved using a shaker (RO-TAP RX-29, W.S. Tyler, OH, USA) equipped with a 2800 μm stainless-steel mesh. Only fractions of <2800 μm in size and with ≥ 80 mg mass loadings were advanced for chemical analysis. Volume-based size distributions of the sieved indoor dust were determined using laser diffraction particle sizing. Across both sites, the dust exhibited a bi-modal volume distribution, with prominent peaks in the 10–50 μm and 100–500 μm size fractions (Fig. S1). In the WL samples, these size fractions accounted for median proportions of 39.6% and 35.3%, respectively, and in the NYC samples, the corresponding values were 39.4% and 36.4%. In contrast, particles smaller than 10 μm and larger than 500 μm comprised a relatively small fraction of the total dust volume at both sites, with median values of approximately 5–6% and 1.8%, respectively. Because dust mass

© 2026 The Author(s). Published by the Royal Society of Chemistry

Environ. Sci.: Adv., 2026, **5**, 866–877 | **867**

distributions scale with volume distributions, entire size-integrated samples were analyzed to assess ingestion rates, which are mass-based metrics. In total, 129 dust samples from 86 homes were characterized: 58 samples from 43 homes in NYC and 71 samples from 43 homes in the WL area. A multi-modal analytical workflow was applied to quantify elemental composition and toxic-metal concentrations and to characterize and quantify EPFR content.

Elemental analysis

First, XRF spectroscopy was used as a non-destructive method to determine the elemental composition of dust for elements heavier than fluorine. This technique is particularly adept at determining quantitative ratios of elements in a sample, making it a valuable tool in the rapid evaluation of dust samples.[24] XRF spectra of dust were acquired on an Epsilon 4 benchtop XRF spectrometer (Malvern Panalytical, Marlborough, MA, USA). Approximately 70 mg of dust was evenly distributed on clean polypropylene films mounted in XRF cups. Omnian™ peak-fitting software was used for element identification and quantitation, and k-means clustering (a machine learning algorithm) was applied to the resulting XRF datasets using previously described code.[25] Cluster separation was evaluated by silhouette analysis (Fig. S2); four identified clusters yielded silhouette scores >0.4, indicating internally coherent groupings.[26] For seasonal analyses discussed later, seasons are denoted as: spring (March 21st – June 19th), summer (June 20th – September 20th), fall (September 21st – December 20th), and winter (December 21st – March 20th). Owing to its non-destructive nature, dust was recovered after XRF analysis for subsequent ICP-MS measurements. XRF yields consistent relative abundances, but absolute quantitation is hindered by matrix effects and complex calibration requirements.[24]

ICP-MS was employed to complement XRF and obtain multi-element quantitation.[27] Targeted analysis included toxicologically relevant toxic metals: Fe, Ni, Cd, Cr, As, Pb, and Cu.[10] For these measurements, ~20 mg aliquots of dust were weighed and transferred to borosilicate digestion vessels (Anton Paar, IL, USA), where 0.5 mL of ultrapure water and 2 mL of ultra-high purity nitric acid (BDH Aristar Ultra, VWR, PA, USA) were added to each sample. Method blanks containing only water and acid were prepared identically. Samples and blanks were then digested simultaneously in an Microwave Digestion System: Multiwave (Anton Parr, IL, USA)using the preset 'Inorganic' program. After digestion, the samples and blanks were brought to a final 50 mL volume with ultrapure water to yield 2.8% (v/v) HNO$_3$. Because Fe concentrations were higher than for other elements, aliquots used for Fe measurements were further diluted 100-fold in HNO$_3$. Analyses were performed on an Element 2 ICP-MS (Thermo Scientific™ Carlsbad, CA, USA) equipped with a Cetac Aridus II nebulizer (Teledyne, OH, USA). Calibration used a multi-element stock standard solution (10 μg mL^{-1} for each element quantified in 2% v/v HNO$_3$; Inorganic Ventures, Christiansburg, VA, USA) with working samples prepared by serial dilution. ICP-MS provided ppt-level

sensitivity with high repeatability, enabling robust quantitation across the target elements.[27]

Because XRF yields robust inter-element ratios, ICP-MS measurements were used to scale XRF-detected elements to absolute concentrations with reasonable accuracy.[24,27] Iron (Fe) served as the internal reference element, owing to its high abundance and ubiquitous presence in all dust samples. Therefore, for element (Y_i) in sample (i), the concentration was estimated as follows:

$$Y_i = \frac{\% \, Y(\text{XRF})_i}{\text{MW}_Y} \times \frac{\text{MW}_{\text{Fe}}}{\% \, \text{Fe}(\text{XRF})_i} \times \text{Fe}(\text{ICPMS})_i \quad (1)$$

where $\% \, Y(\text{XRF})_i$ and $\% \, \text{Fe}(\text{XRF})_i$ are XRF mass fractions (wt%), MW denotes atomic weight, and $\text{Fe}(\text{ICPMS})_i$ is the Fe concentration determined by ICP-MS. The reliability of this methodology is illustrated in Fig. 1, showcasing a selected sample from the WL area: ICP-MS values (red) and XRF-scaled estimates (blue) within a factor of two, with slight overestimation for Cr and underestimation for Cu. Similarly, adequate agreement was observed across all dust samples (Fig. S3), supporting the use of XRF ratios for screening-level quantification.

Elemental enrichment factors (EFs) for element (Y_i) in sample (i) relative to Earth's crust were calculated following established methods,[28,29] using Mn as the conservative reference element due to its ubiquity in all dust samples and linkage to crustal sources.[28]

$$\text{EF}_{Y,i} = \left(\frac{\text{Conc}_Y}{\text{Conc}_{\text{Mn}}} \right)_{\text{Dust},i} \bigg/ \left(\frac{\text{Conc}_Y}{\text{Conc}_{\text{Mn}}} \right)_{\text{Earth's crust}} \quad (2)$$

Earth's crustal element abundances were taken from published compilations.[30] Values of $\text{EF}_Y > 2$ suggested anthropogenic enrichment attributable to either indoor or regional outdoor sources.
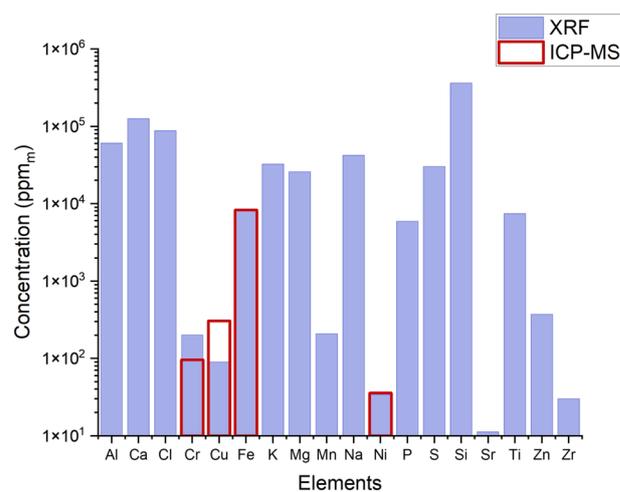

Fig. 1 Elemental analysis of a representative house-dust sample integrating XRF and ICP-MS datasets. Absolute metal concentrations determined by ICP-MS (red) and estimated from XRF inter-elemental ratios (blue). Cr, Cu, and Ni were quantified by both methods; Fe was measured by ICP-MS and used as the anchor element to scale XRF ratios to absolute concentrations.

Mapping and spatial autocorrelation of elemental concentrations were performed in ArcGIS Pro™ software (v 3.4). Global Moran's index (I) was computed for indexed dimensions i and j based on the latitude and longitude of the collected dust samples.

$$I = \frac{1}{\sum_{ij} w_{ij}} \frac{\sum_{ij} w_{ij}\left(X_i - \overline{X}\right)\left(X_j - \overline{X}\right)}{N^{-1}\sum_i \left(X_i - \overline{X}\right)^2} \tag{3}$$

Here, N is the number of observations, X_i is the value at location i, $\overline{X}$ is the sample mean, and w_{ij} are elements of the spatial-weights matrix. Values of $I < 0$ indicate negative spatial autocorrelation (dispersion), $I > 0$ indicate positive spatial autocorrelation (clustering), and $I \approx 0$ indicates spatial randomness; within the ranges of $-1 < I < 0$ and of $0 < I < 1$, more negative or more positive values, respectively, reflect stronger dispersion or clustering and a tighter linkage to localized sources[22,31]

EPFR characterization

EPR spectroscopy was used to detect and quantify EPFRs in dust samples. Approximately 5–10 mg of dust material was loaded into quartz capillary tubes and inserted into standard EPR tubes. Spectra were acquired with a EMX Plus X-band EPR spectrometer (9.85 GHz, Bruker, MA, USA) with the following settings: microwave power 2 mW, modulation frequency 100 kHz, modulation amplitude 5 G, center field 3516 G, conversion time 6 ms, time constant of 0.64 ms, 1024 points per scan, and 4 scans averaged. Sweep widths of 250, 500, or 1000 G were selected depending on the sample and radicals present.

Absolute spin quantification was performed using the spin-counting routine in Bruker's WinEPR software, which converts the double integral of the first-derivative spectrum to a spin count. Instrument response was calibrated using 4-hydroxy-2,2,6,6-tetramethylpiperidin-1-oxyl (TEMPOL, 98% purity, TCI, Tokyo, Japan) measured under identical parameters at each sweep width. Sample spin counts were obtained by scaling the sample double integral to the TEMPOL calibration and normalizing by sample mass to report concentrations as radicals μg^{-1} dust. Quality control and assurance protocols for collection and analytical methodology are provided in SI Note 1.

Results and discussion

Elemental concentrations were quantified to compare rural and urban samples. Fig. 2 shows absolute concentrations of elements exceeding 0.5 $\mu g\ g^{-1}$ of dust (ppm_m) (urban NYC, green; rural, WL, purple). In the box-and-whisker plots, the central line denotes the mean, and whiskers indicate the observed range. Most elements are elevated in rural dust, particularly crustal constituents (Na, Al, Si, Mg, P, S, Cl, K, Ca, Ti, Fe, and Mn).[32] However, several toxicologically relevant elements (Ni, Pb, Cu, and Zn) are enhanced in urban dust, underscoring the need for region-specific assessment of indoor exposure hazards.

These urban enrichments align with prior reports.[2] Typically, outdoor and indoor sources jointly shape toxic metal burdens
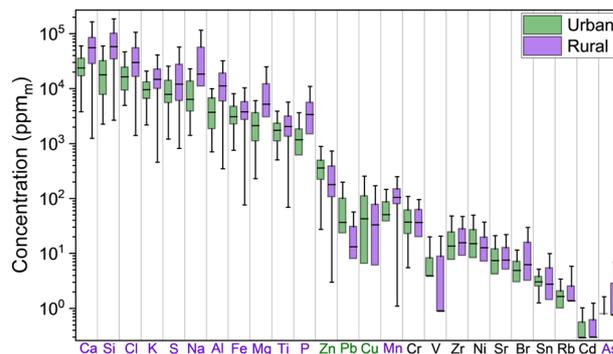

Fig. 2 Box-and-whisker plot of element concentrations in house dust derived from combined ICP-MS and XRF measurements. Green denotes samples from NYC; purple denotes samples from WL. Element labels are color-coded to indicate the direction of the regional difference: green (NYC > WL), purple (WL > NYC), black ($\approx$ equal). The central lines indicate the mean; whiskers show the observed range. The mean and median values presented in the plot are listed in Table S1.

and regional contrasts. Elevated Pb is commonly associated with traffic and industrial activities and with legacy indoor sources such as lead-based paint and plumbing, especially in the older housing (<1960s in the United States) prevalent in NYC.[33,34] Zn and Pb contributions likely arise from tire wear and galvanized automotive parts, and Zn is naturally present in soil.[2,29] Prior work indicates that Zn and Cu are frequently linked with industrial processes such as smelting and combustion.[35] Among low concentration elements (<10^3 ppm_m), mean concentrations of Mn and As were higher in rural samples (WL). Mn is associated with oxidative stress, EPFR formation (discussed below), and neurotoxicity.[36,37] In these samples, Mn exhibited a broader concentration range in rural dust than urban dust, plausibly consistent with transfer from outdoor fungicide use; indoor burdens depend on cleaning practices, occupation of residents, and proximity to treated land.[36] Elevated As in rural areas is likely consistent with agricultural inputs (pesticides and fertilizers)[2] and with geogenic contributions from Indiana bedrock, which elevates As in local soils and waters.[38] These location-dependent patterns underscore the need for region-specific assessment of toxic metals in house dust to inform exposure evaluation. Room-to-room differences were also observed. ICP-MS results (Fig. S5) indicate that some metals likely tracked indoors from outdoor sources (Fe, Pb, Cr, Cd) were elevated in entryways, whereas others with stronger indoor source contributions (As, Ni, Cu) were more uniformly distributed across living/common rooms and infant bedrooms.

Fig. 3 shows elemental enrichment factors ($EF_{Y,i}$) relative to Mn (set as a reference) used to identify non-crustal sources.[12,28,39,40] By convention, EF > 2 indicates enrichment above crustal background, and EF > 10 denotes strong enrichment. Notably, the $EF_{Y,i}$ values need to be considered cautiously because Mn may have non-crustal inputs from anthropogenic sources (e.g., methylcyclopentadienyl manganese tricarbonyl in gasoline and subsequent vehicle exhaust, Mn-based fungicides, brake wear, welding emissions, etc.), especially in a very
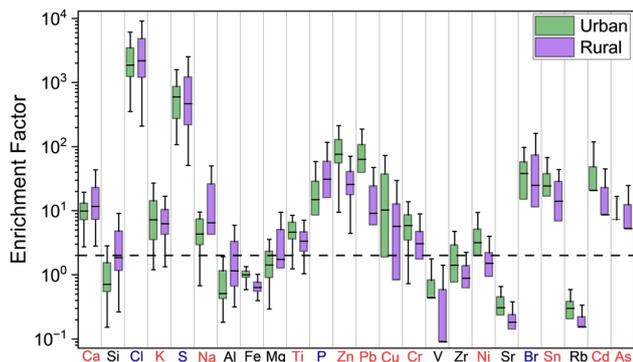
Fig. 3 Enrichment factors (EFs) for elements in house dust from urban (NYC, green) and rural (WL, purple) residences. The dashed line at EF = 2 marks enrichment above crustal background; elements above this threshold are highlighted in red to indicate likely anthropogenic or regionally enhanced contributions. Elements marked in blue are common constituents of organic compounds and may reflect natural or biogenic sources. EFs are referenced to Mn. The mean and median values presented in the plot are listed in Table S2.

complex urban environment such as NYC. Therefore, the potentially elevated Mn level breaks the conservative tracer assumption, which mask true enrichment of other elements (deflating their EFs) and bias source apportionment toward crustal origins. Nevertheless, very large EFs > 10 for Cl, S, P, and Br are consistent with diverse input from organic compounds of

both natural and anthropogenic origins. Elements primarily associated with inorganic species, such as Ca, K, Na, Ti, Cu, Cr, Ni, and As, are also enriched, implicating both indoor sources and outdoor-to-indoor transfer. The most pronounced EFs were observed for Zn, Pb, Sn, and Cd, which were heavily enriched. These patterns reasonably align with established source profiles – paints, building materials, industrial, and traffic-related emissions for Zn and Pb;[28,33,34] mining, smelting, pigments, and agricultural inputs for Cd (crustal ≈ 0.2 ppm$_m$);[41] and jewelry, pigments, and solder for Sn.[42] Overall, EF assessments highlight elements most influenced by non-crustal inputs and prioritize Zn, Pb, Sn, and Cd for toxicological evaluation due to their high enrichment and hazard potential.

Natural-source elements were examined to trace dust accumulation pathways and sources of resuspended particulate matter. K-means clustering separates dust samples within similar elemental composition into groups, summarized by cluster centroids. This approach enables the whole-scale comparison of composition trends across regions and seasons without relying on individual-element concentrations. Fig. 4 reports centroid-specific elemental ratios (each element relative to the total signal) for constituents contributing >0.5% of the total. Four distinct clusters were identified and provisionally labeled by plausible contributors: clays (brown; elevated Si, Cl, K, Fe, Ca), salt (blue; enriched Na and Cl), sand (pink; high Si), and concrete (grey; elevated Ca consistent with CaO-rich cement). In contrast to the toxic-metal patterns discussed
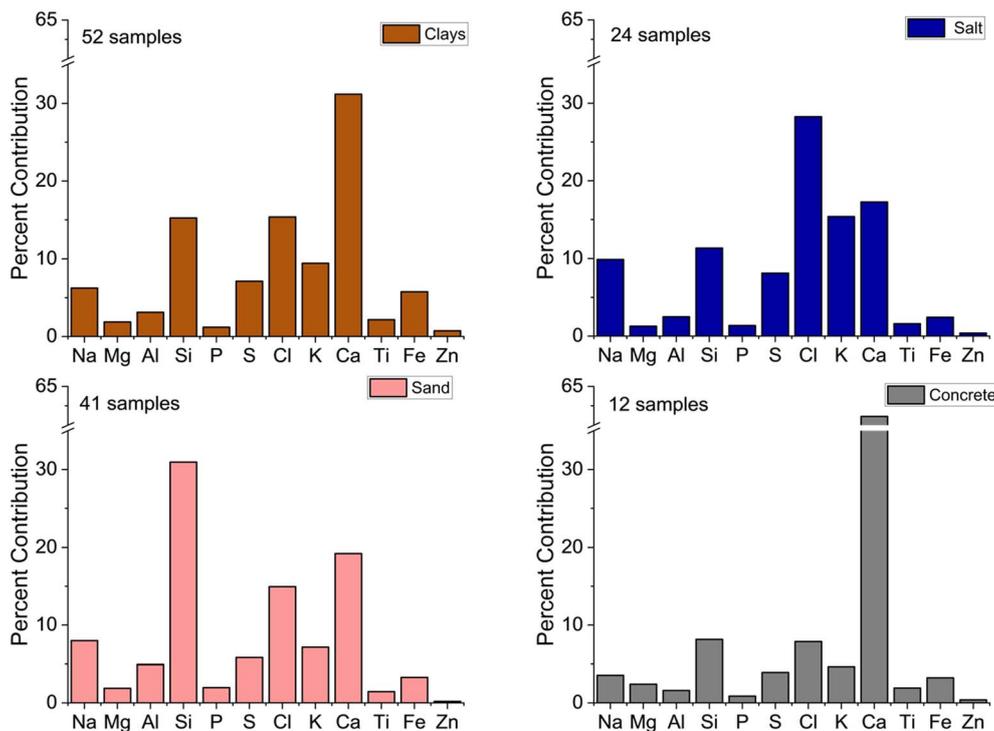

Fig. 4 K-means clustering of XRF elemental-ratio profiles for house dust samples. Panels show relative elemental fractions corresponding to each of four cluster centroids (only elements >0.5% are shown); panel titles report the number of samples (n) assigned to each of the clusters and the corresponding descriptor legends: clays, salt, sand, and concrete. Results of the Silhouette analysis indicated efficient clustering with average silhouette values of >0.4 (Fig. S4).
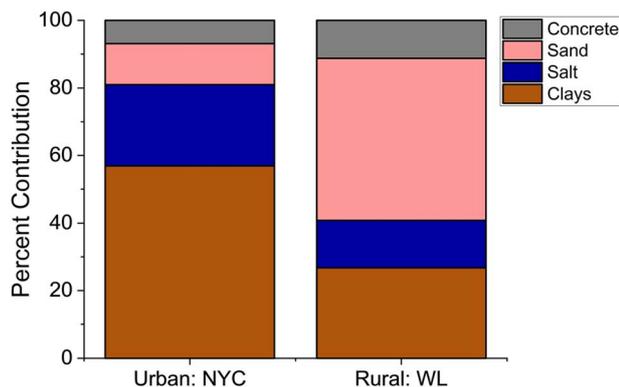
Fig. 5 Fractions (Percent Contributions) of dust samples attributed to four identified compositional clusters. Stacked bars show the contributions from each cluster to samples from urban (NYC) and rural (WL) residences.

above, these clusters are dominated by naturally abundant elements and are expected to vary primarily with outdoor sources (*e.g.*, soil/mineral dust, salts) and building materials.[2,32] For clarity, these compositional clusters are hereafter referred to as clays, salt, sand, and concrete, with the understanding that these source labels are operationally defined.

Fig. 5 summarizes fractions of dust samples from rural (WL) and urban (NYC) households attributed to the identified clusters – concrete, sand, salt, and clays. A predominance of sand-type dust in WL is consistent with regional soils derived from sandy deposits in this part of Indiana.[43] NYC samples show a larger fraction of clays or mixed-composition dust, consistent with the heterogeneous, bioengineered character of urban soils and the diversity of urban dust sources (*e.g.*, soils, landfills, traffic, and infrastructure wear).[44,45] Across both regions, soil-related dust (clays and sand) samples account for >60%, with the remaining ~40% attributed to concrete- and salt-like dust. The higher proportion of salt-like dust samples in NYC is plausibly influenced by marine aerosol from the adjacent ocean

and harbor, which contributes to particulate matter in coastal cities and can be transferred indoors.[46] Concrete-like dust appears in both regions at similar relative fractions, consistent with common building material inputs.[2]

Fig. 6 illustrates seasonal differences in dust composition with samples grouped by the season of collection. Overall, samples from NYC exhibited weaker seasonality than samples from WL. Prior studies reported sea-salt contributions to particulate matter in NYC during warmer months owing to seasonal wind patterns, consistent with the observed increase in salt-like dust in summer and fall.[47] In contrast, WL dust showed pronounced seasonality. A marked increase in sand-like samples was observed in summer, plausibly reflecting increased tracking of soil/dirt with greater outdoor activity, and contributions from agricultural operations (planting/harvesting) that loft mineral dust in spring-summer.[48,49] Salt-like dust also increased in WL during winter, consistent with regional road-salt application. The concurrent decrease in NYC suggests distinct sources for compositionally similar salt-like dust in the two regions (marine aerosol *vs.* de-icing salts). These seasonal and source differences underscore the complexity of indoor environments and the need for context-specific source attribution when evaluating elemental drivers of toxicity.

Fig. 7 lists the elements with a significant positive Moran's index ($I > 0.05$) calculated for the elements observed in urban and rural regions, highlighting the strength of spatial clustering in each region. Corresponding geospatial concentration maps are provided in Fig. S6–S19. In NYC, a significant clustering and therefore influence of localized sources were observed for Si, Cl, Na, K, P, Al, Ti, S, and Br. In WL, more elements were found to cluster geospatially: K, Cu, Si, S, Ca, Pb, Ti, Al, Rb, Zn, Na, P, Mg, Sr, As, Cl, and Zr. These patterns suggest regional localized hotspots consistent with outdoor influences (*e.g.*, traffic, industry, soils, or marine aerosol). Elements' spatial autocorrelation is more likely to be dominated by indoor sources or by building-specific variability. Illustrative cases include spatial clustering of Pb in downtown Lafayette, consistent with traffic
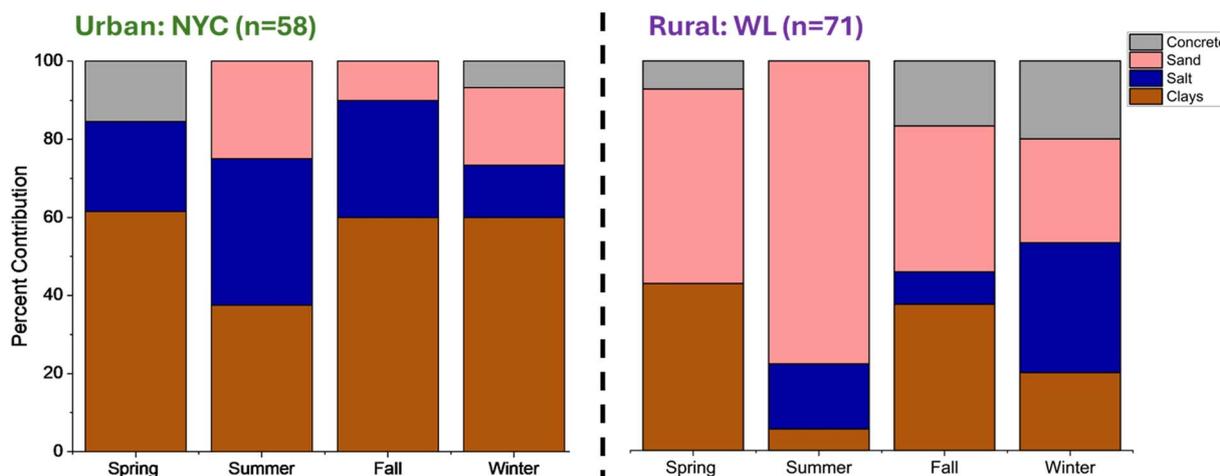

Fig. 6 Seasonal distribution of compositional clusters by region. Stacked bars show the overall contributions from each cluster to dust samples from urban (NYC) and rural (WL) residences across spring, summer, fall, and winter.
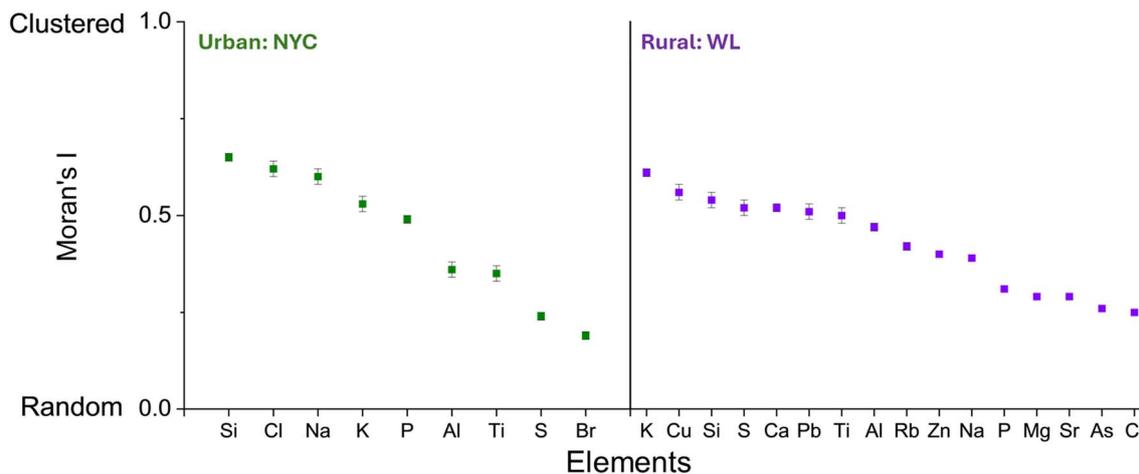
© 2026 The Author(s). Published by the Royal Society of Chemistry

Environ. Sci.: Adv., 2026, **5**, 866–877 | **871**

Fig. 7 Positive Moran's Index (I) values elements exhibiting significant spatial autocorrelation in NYC (left panel) and WL (right panel). Symbols and error bars indicate the I values and their variances, respectively. Elements not shown did not display significant clustering (*i.e.*, $I \approx 0$). Values were identified to be significant if the *p*-value < 0.05.

and building-related inputs, whereas in NYC Pb is likely more dependent on building age and construction.[33] Elevated Cu in southwest Lafayette aligns with nearby industrial activity. In NYC, Na concentrations are higher in Manhattan than in Brooklyn and Queens, consistent with harbor proximity. Notably, fewer elements are autocorrelated in NYC overall; among enriched elements, only Ti and Na show clustering, suggesting that many anthropogenic metals arise from diffuse indoor sources or highly localized activities rather than broad regional inputs.

Infant risk from occasional ingestion of dust-borne metals was screened using hazard quotient (HQ = ADD/RfD) and lifetime cancer risk (LCR = ADD × SF) factors, where ADD is an average daily dose, SF is a metal specific cancer slope factor (SF), and RfD is the element specific reference dose set by the EPA[10] scale metal concentration by ingestion rate and body weight. Further details of the screening methodology as well as tabulated HQ and LCR values are included in the SI file (SI Note 2). All HQ factors for Al, As, Cd, Cr, Cu, Fe, Ni, Pb, and Zn were <1 in both regions, suggesting no hazard concern for sampled households. Similarly, LCR factors were at or below 10^{-4}, which is within the range considered as low-level carcinogenic risk.

Measurable EPFR signals were detected by EPR in 67% of urban dust (NYC) samples and 77% of rural dust (WL) samples. Fig. 8 illustrates representative EPFR types observed in this study. Additional EPR signatures of dust frequently appeared as overlapping spectra with variable line shapes, often showing attenuation of the central peak relative to outer peaks, consistent with spectral overlap or powder anisotropy and motivating the whole-spectrum spin-quantification approach described above. The most prevalent signal (Fig. 8a) was a single broad peak with $g = 2.001$–2.007, detected in 72% of samples above the detection limit (10^9 radicals μg^{-1} dust). This feature is characteristic of combustion-related EPFRs and is consistent with inputs from cooking, outdoor burning, or tobacco smoking.[16,50,51] Slightly elevated *g*-values relative to typical organic-centered EPFRs[50,51] are plausibly explained by interactions in metal-rich dust, wherein electron transfer at the metal oxide surfaces can generate and stabilize surface-bound organic radicals, shifting *g* upward.[19] A second recurring pattern was a triplet centered at $g \approx 2.013$ with ~43 *G* splitting (Fig. 8b), similar to O-centered radical signatures reported for indoor dust.[52] A third common pattern was a sextet centered at $g \approx 2.005$ with ~88 *G* splitting (Fig. 8c), attributable to Mn^{2+}
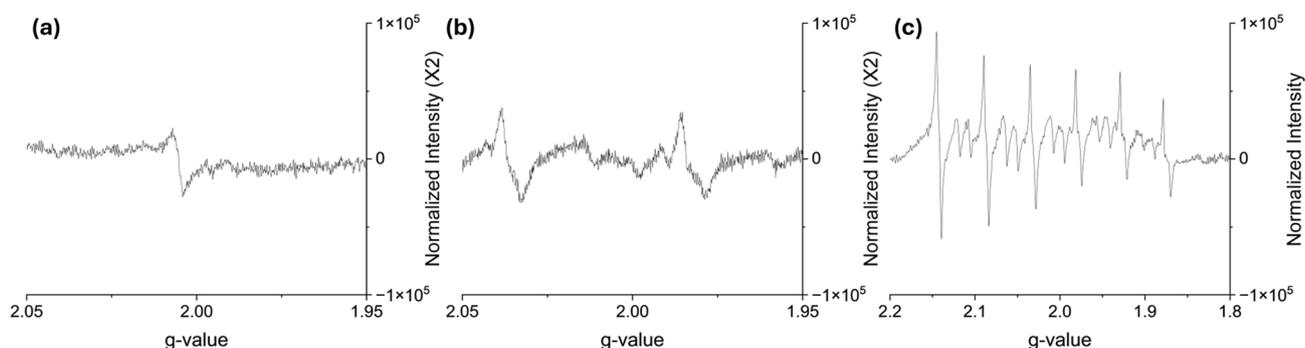

Fig. 8 Representative EPR spectra, normalized by dust-sample mass: (a) combustion-associated radical (broad single line, $g = 2.001$–2.007);[54] (b) O-centered radical (triplet, $g \approx 2.013$, ~43 G splitting);[52] (c) Mn^{+2}-associated radical (sextet, $g \approx 2.005$, ~88 G hyperfine splitting).[53]
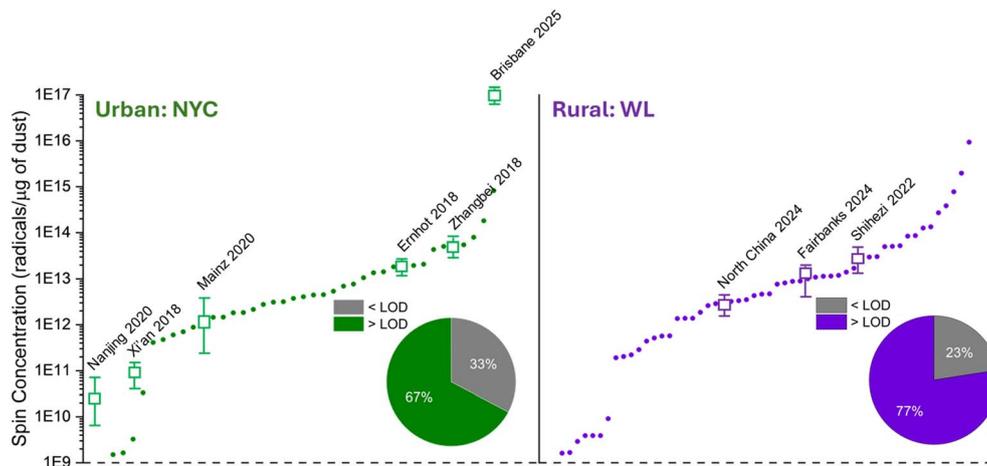
Fig. 9 EPFR concentrations in house dust (radicals μg^{-1} dust) for samples above the detection limit (10^9 radicals μg^{-1} of dust) in urban (NYC) and rural (WL) residences. Literature ranges from urban,[52,54–57] and rural[51,58,59] dust/particulate matter are overlaid for context. Pie charts report the proportion of samples in each region with a detectable *versus* non-detectable EPFR signal.

hyperfine coupling associated with carbon-centered radicals in soil or lignin from biomass burning.[50,53] Consistent with a metal-stabilization mechanism,[13] Mn concentration was positively associated with the corresponding spin concentration across the dataset (Fig. S20). This Mn-linked sextet appeared in 7 of 129 samples (six rural, one urban), motivating future expanded sampling to resolve metal–EPFR coupling across environments.

Fig. 9 reports total EPFR concentrations quantified from EPR measurements using TEMPOL-calibrated spin counting. Measurements below the limit of detection (10^9 radicals μg^{-1} dust) were excluded. The pie charts show the percentage of dust samples with detectable EPRFs; detected concentrations span $\sim10^9$–10^{16} radicals μg^{-1} dust in both regions. Similar magnitudes and distribution patterns suggest predominantly indoor/behavioral sources, with outdoor contributions superimposed. The observed range aligns with prior reports for urban[52,54–57] and rural[51,58,59] dust and particulate matter. Toxicological interpretation remains constrained by limited EPFR-specific benchmarks. No regulatory guideline exists for EPRF levels in indoor dust, although EPFRs generate ROS in biological media and have been linked to inflammation, oxidative stress, and cardiopulmonary effects.[17] In a roundworm model, EPFRs with concentrations of $\sim10^{17}$ radicals μg^{-1} dust produced measurable neurotoxicity and oxidative stress after 24 h exposure.[60] Reported EPFR concentrations here are at least an order of magnitude lower, suggesting limited acute concern. However, uncertainties in bio-accessibility in relevant fluids, co-exposure with metals, and chronic, low-dose exposure (particularly for infants) warrant caution and targeted follow-up studies.

Conclusions

A screening framework for indoor dust was established that couples elemental profiling with EPFR quantification to assess toxicity and probe indoor chemistry. Region-specific differences were observed: many metals were higher in rural dust, but several toxic metals (Zn, Pb, Cu) were elevated in urban samples, and Zn, Pb, Cd, and Sn were consistently heavily enriched, indicating strong anthropogenic inputs. Soil-type contrasts (clay-rich *vs.* sandy) and seasonal signatures differentiated salt sources – marine influence in New York City *vs.* winter deicing in West Lafayette, underscoring the need for localized studies. Spatial analysis (Moran's I) identified hotspots suggestive of traffic, industrial, and infrastructure-related sources. Risk screening indicated that average hazard quotients were <1.5 and potential cancer risks below 10^{-4} for both regions. However, due to the variation exhibited between NYC and WL regions, additional work may need to be done to examine additional regions and confirm the lack of risk. EPFRs were detected in more than two-thirds of the dust samples with concentrations spanning $\sim10^9$–10^{16} radicals μg^{-1} and EPR spectra consistent with combustion- and metal-associated radicals. Metal-rich matrices likely stabilized EPFRs, reinforcing their persistence and potential to generate ROS.

This study presented a targeted framework for assessing the toxicity of house dust that may be ingested by infants, quantifying toxic metals and EPFRs using screening techniques. Chemical differences between house dust collected in WL and NYC are evaluated to infer source difference and species of elevated concern. EPFR concentrations and radical types are characterized in both rural and urban dust, highlighting EPFRs as an emerging pollutant. Although spatially localized metal hotspots were identified, more spatially balanced sampling across each region would enable finer source apportionment. Because EPFRs are complex and their toxicological benchmarks (especially for ingestion) remain limited, additional studies are needed to refine exposure metrics and hazard evaluation in indoor dust.[20] Given their ubiquity and suspected role in multiphase reactivity, source apportionment, bio-accessibility, and dose–response relationships, EPFRs (along with co-occurring metals) should be prioritized to refine exposure assessments and inform indoor environmental health

© 2026 The Author(s). Published by the Royal Society of Chemistry

Environ. Sci.: Adv., 2026, **5**, 866–877 | **873**

interventions. Ongoing work focuses on integrating video-based behavior analysis, advanced dust characterization, and mass-balance modeling to better quantify infant dust ingestion and inhalation for more refined risk assessments.

Additional regional studies are warranted, as this work revealed markable differences in toxic metals profiles between WL and NYC. Individualized assessments of infant dust ingestion incorporating body size, dust-ingestion rates, inhalation rates, and the toxicity of resuspended airborne particles, are needed to refine risk estimates. Given the high transition-metal content of house dust, the role of metals in EPFR formation and persistence should also be investigated under physiologically relevant conditions (*e.g.*, surrogate lung fluid, saliva, esophageal matrices) to better constrain oxidative-stress potential from dust ingestion and inhalation.

Author contributions

E. H. and A. L. conceptualized the project and performed visualization, data collection, and writing of the document. S. S. performed data analysis and visualization of maps and spatial autocorrelation. K. M., P.·C., L. H., and T. N. collected and analyzed XRF and EPR datasets. C. W. developed the methodology and conceptualized some of the project. S. P. and B. M. performed dust sample preparation. P. T. collected dust samples in West Lafayette, I. N. O. H., M. K., and M. S. collected dust samples in New York City. B. B., L. C., K. A., and A. L. acquired funding, conceptualized the project, and supervised.

Conflicts of interest

There are no conflicts to declare.

Data availability

Data for this article, including all sample IDs, locations and collection information, EPR concentrations, XRF clustering IDs, individual elemental concentrations, and Moran's index values used are available at Purdue University Research Repository at https://purr.purdue.edu/projects/lafnycdust/.

Supplementary information (SI) is available. See DOI: https://doi.org/10.1039/d5va00477b.

Acknowledgements

References

1 J. P. D. Abbatt and C. Wang, The Atmospheric Chemistry of Indoor Environments, *Environ. Sci.: Processes Impacts*, 2020, **22**(1), 25–48, DOI: 10.1039/C9EM00386J.

2 A. Araja, M. Bertins, G. Celma, L. Busa and A. Viksna, Distribution of Minor and Major Metallic Elements in Residential Indoor Dust: A Case Study in Latvia, *Int. Res. J. Publ. Environ. Health*, 2023, **20**(13), 6207, DOI: 10.3390/ijerph20136207.

3 W. D. Fahy, F. Wania and J. P. D. Abbatt, When Does Multiphase Chemistry Influence Indoor Chemical Fate?, *Environ. Sci. Technol.*, 2024, **58**(9), 4257–4267, DOI: 10.1021/acs.est.3c08751.

4 K. Somsunun, T. Prapamontol, T. Kuanpan, T. Santijitpakdee, K. Kohsuwan, N. Jeytawan and N. Thongjan, Health Risk Assessment of Heavy Metals in Indoor Household Dust in Urban and Rural Areas of Chiang Mai and Lamphun Provinces, Thailand, *Toxics*, 2023, **11**(12), 1018, DOI: 10.3390/toxics11121018.

5 J. Cohen, H. Hubbard, H. Özkaynak, K. Thomas, L. Phillips and N. Tulve, Meta-Analysis of Soil and Dust Ingestion Studies, *Environ. Res.*, 2024, **261**, 119649, DOI: 10.1016/j.envres.2024.119649.

6 T. Wu, M. Fu, M. Valkonen, M. Täubel, Y. Xu and B. E. Boor, Particle Resuspension Dynamics in the Infant Near-Floor Microenvironment, *Environ. Sci. Technol.*, 2021, **55**(3), 1864–1875, DOI: 10.1021/acs.est.0c06157.

7 J. A. Rosati, J. Thornburg and C. Rodes, Resuspension of Particulate Matter from Carpet Due to Human Activity, *Aerosol Sci. Technol.*, 2008, **42**(6), 472–482, DOI: 10.1080/02786820802187069.

8 A. Roy, A. K. Jha, A. Kumar, T. Bhattacharya, S. Chakraborty, N. P. Raval and M. Kumar, Heavy Metal Pollution in Indoor Dust of Residential, Commercial, and Industrial Areas: A Review of Evolutionary Trends, *Air Qual. Atmos. Health*, 2024, **17**(4), 891–918, DOI: 10.1007/s11869-023-01478-y.

9 M. Jaishankar, T. Tseten, N. Anbalagan, B. B. Mathew and K. N. Beeregowda, Toxicity, Mechanism and Health Effects of Some Heavy Metals, *Interdiscip. Toxicol.*, 2014, **7**(2), 60–72, DOI: 10.2478/intox-2014-0009.

10 S. Y. Tan, S. M. Praveena, E. Z. Abidin and M. S. Cheema, A Review of Heavy Metals in Indoor Dust and Its Human Health-Risk Implications, *Rev. Environ. Health*, 2016, **31**(4), 447–456, DOI: 10.1515/reveh-2016-0026.

11 T. D. Sowers, C. M. Nelson, G. L. Diamond, M. D. Blackmon, M. L. Jerden, A. M. Kirby, M. R. Noerpel, K. G. Scheckel, D. J. Thomas and K. D. Bradham, High Lead Bioavailability of Indoor Dust Contaminated with Paint Lead Species, *Environ. Sci. Technol.*, 2021, **55**(1), 402–411, DOI: 10.1021/acs.est.0c06908.

12 J. H. Dingle, L. Kohl, N. Khan, M. Meng, Y. A. Shi, M. Pedroza-Brambila, C.-W. Chow and A. W. H. Chan, Sources and Composition of Metals in Indoor House Dust in a Mid-Size Canadian City, *Environ. Pollut.*, 2021, **289**, 117867, DOI: 10.1016/j.envpol.2021.117867.

13 M. W. Tehrani, E. C. Fortner, E. S. Robinson, A. A. Chiger, R. Sheu, B. S. Werden, C. Gigot, T. Yacovitch, S. V. Bramer, T. Burke, K. Koehler, K. E. Nachman, A. M. Rule and P. F. DeCarlo, Characterizing Metals in Particulate Pollution in Communities at the Fenceline of Heavy Industry: Combining Mobile Monitoring and Size-Resolved Filter Measurements, *Environ. Sci.: Processes Impacts*, 2023, **25**(9), 1491–1504, DOI: 10.1039/D3EM00142C.

14 W. Gehling and B. Dellinger, Environmentally Persistent Free Radicals and Their Lifetimes in PM2.5, *Environ. Sci. Technol.*, 2013, **47**(15), 8172–8178, DOI: 10.1021/es401767m.

15 S. L. Baum, I. G. M. Anderson, R. R. Baker, D. M. Murphy and C. C. Rowlands, Electron Spin Resonance and Spin Trap Investigation of Free Radicals in Cigarette Smoke: Development of a Quantification Procedure, *Anal. Chim. Acta*, 2003, **481**(1), 1–13, DOI: 10.1016/S0003-2670(03)00078-3.

16 F. Hasan, L. Khachatryan and S. Lomnicki, Comparative Studies of Environmentally Persistent Free Radicals on Total Particulate Matter Collected from Electronic and Tobacco Cigarettes, *Environ. Sci. Technol.*, 2020, **54**(9), 5710–5718, DOI: 10.1021/acs.est.0c00351.

17 T. Dugas, S. Lomnicki, S. Cormier, B. Dellinger and M. Reams, Addressing Emerging Risks: Scientific and Regulatory Challenges Associated with Environmentally Persistent Free Radicals, *Int. J. Environ. Res. Public Health.*, 2016, **13**(6), 573, DOI: 10.3390/ijerph13060573.

18 L. W. Kiruri, L. Khachatryan, B. Dellinger and S. Lomnicki, Effect of Copper Oxide Concentration on the Formation and Persistency of Environmentally Persistent Free Radicals (EPFRs) in Particulates, *Environ. Sci. Technol.*, 2014, **48**(4), 2212–2217, DOI: 10.1021/es404013g.

19 S. Liu, G. Liu, L. Yang, D. Li and M. Zheng, Critical Influences of Metal Compounds on the Formation and Stabilization of Environmentally Persistent Free Radicals, *Chem. Eng. J.*, 2022, **427**, 131666, DOI: 10.1016/j.cej.2021.131666.

20 E. P. Vejerano, G. Rao, L. Khachatryan, S. A. Cormier and S. Lomnicki, Environmentally Persistent Free Radicals: Insights on a New Class of Pollutants, *Environ. Sci. Technol.*, 2018, **52**(5), 2468–2481, DOI: 10.1021/acs.est.7b04439.

21 A. Phaniendra, D. B. Jestadi and L. Periyasamy, Free Radicals: Properties, Sources, Targets, and Their Implication in Various Diseases, *Indian J. Clin. Biochem.*, 2015, **30**(1), 11–26, DOI: 10.1007/s12291-014-0446-0.

22 Y. Chen, Spatial Autocorrelation Equation Based on Moran's Index, *Sci. Rep.*, 2023, **13**(1), 19296, DOI: 10.1038/s41598-023-45947-x.

23 E. B. Brandon, K. Adolph, L. Claxton, A. Laskin, O. Herzberg, P. Thompson, S. Patra, B. Magnuson and E. R. Halpern, A Transdisciplinary Process-Oriented Approach to Evaluate Infant Exposure to Indoor Dust, *J. Expo. Sci. Environ. Epidemiol.*, 2026, DOI: 10.1038/s41370-025-00823-w.

24 E. Marguí, I. Queralt and E. de Almeida, X-Ray Fluorescence Spectrometry for Environmental Analysis: Basic Principles, Instrumentation, Applications and Recent Trends, *Chemosphere*, 2022, **303**, 135006, DOI: 10.1016/j.chemosphere.2022.135006.

25 R. C. Moffet, H. Furutani, T. C. Rödel, T. R. Henn, P. O. Sprau, A. Laskin, M. Uematsu and M. K. Gilles, Iron Speciation and Mixing in Single Aerosol Particles from the Asian Continental Outflow, *J. Geophys. Res. Atmos.*, 2012, **117**(D7), 204, DOI: 10.1029/2011JD016746.

26 H. Lai, T. Huang, B. Lu, S. Zhang and R. Xiaog, Silhouette Coefficient-Based Weighting k-Means Algorithm, *Neural Comput. Appl.*, 2025, **37**(5), 3061–3075, DOI: 10.1007/s00521-024-10706-0.

27 M. Balcerzak, Mass Spectrometric Detectors for Environmental Studies, in *Application of IC-MS and IC-ICP-MS in Environmental Research*; John Wiley & Sons, Ltd, 2016, pp. 47–78, DOI: 10.1002/9781119085362.ch2.

28 C. F. Isley, K. L. Fry, X. Liu, G. M. Filippelli, J. A. Entwistle, A. P. Martin, M. Kah, D. Meza-Figueroa, J. T. Shukle, K. Jabeen, A. O. Famuyiwa, L. Wu, N. Sharifi-Soltani, I. N. Y. Doyi, A. Argyraki, K. F. Ho, C. Dong, P. Gunkel-Grillon, C. M. Aelion and M. P. Taylor, International Analysis of Sources and Human Health Risk Associated with Trace Metal Contaminants in Residential Indoor Dust, *Environ. Sci. Technol.*, 2022, **56**(2), 1053–1068, DOI: 10.1021/acs.est.1c04494.

29 M. Wang, Y. Lv, X. Lv, Q. Wang, Y. Li, P. Lu, H. Yu, P. Wei, Z. Cao and T. D. An, Sources and Health Risks of Heavy Metals in Indoor Dust across China, *Chemosphere*, 2023, **313**, 137595, DOI: 10.1016/j.chemosphere.2022.137595.

30 S. R. Taylor, Abundance of Chemical Elements in the Continental Crust: A New Table, *Geochim. Cosmochim. Acta*, 1964, **28**(8), 1273–1285, DOI: 10.1016/0016-7037(64)90129-2.

31 C. Schmal, J. Myung, H. Herzel and G. Bordyugov, Moran's I Quantifies Spatio-Temporal Pattern Formation in Neural Imaging Data, *Bioinformatics*, 2017, **33**(19), 3072–3079, DOI: 10.1093/bioinformatics/btx351.

32 M. Fleischer, The Abundance and Distribution of the Chemical Elements in the Earth's Crust, *J. Chem. Educ.*, 1954, **31**(9), 446, DOI: 10.1021/ed031p446.

33 D. O'Connor, D. Hou, J. Ye, Y. Zhang, Y. S. Ok, Y. Song, F. Coulon, T. Peng and L. Tian, Lead-Based Paint Remains a Major Public Health Concern: A Critical Review of Global Production, Trade, Use, Exposure, Health Risk, and Implications, *Environ. Int.*, 2018, **121**, 85–101, DOI: 10.1016/j.envint.2018.08.052.

34 A. E. Nigra, W. Lieberman-Cribbin, B. C. Bostick, S. N. Chillrud and D. Carrión, Geospatial Assessment of Racial/Ethnic Composition, Social Vulnerability, and Lead Water Service Lines in New York City, *Environ. Health Perspect.*, 2023, **131**(8), 087015, DOI: 10.1289/EHP12276.

35 R. O. Gonzalez, S. Strekopytov, F. Amato, X. Querol, C. Reche and D. Weiss, New Insights from Zinc and Copper Isotopic Compositions into the Sources of Atmospheric Particulate Matter from Two Major European Cities, *Environ. Sci. Technol.*, 2016, **50**(18), 9816–9824, DOI: 10.1021/acs.est.6b00863.

36 R. Gunier, M. Jerrett, D. Smith, T. Jursa, P. Yousefi, J. Camacho, A. Hubbard, B. Eskenazi and A. Bradman, Determinants of Manganese Levels in House Dust Samples from the CHAMACOS Cohort, *Sci. Total Environ.*, 2014, 360–368, DOI: 10.1016/j.scitotenv.2014.08.005.

37 L. Li and X. Yang, The Essential Element Manganese, Oxidative Stress, and Metabolic Diseases: Links and Interactions, *Oxid. Med. Cell. Longev.*, 2018, **2018**, 7580707, DOI: 10.1155/2018/7580707.

© 2026 The Author(s). Published by the Royal Society of Chemistry

Environ. Sci.: Adv., 2026, **5**, 866–877 | **875**

38 S. Letsinger Geological Investigations of the Distribution of Arsenic in Indiana Groundwater; 2017. doi: DOI: 10.13140/RG.2.2.25066.29123.

39 H. K. Gul, G. Gullu, P. Babaei, A. Nikravan, P. B. Kurt-Karakus and G. Salihoglu, Assessment of House Dust Trace Elements and Human Exposure in Ankara, Turkey, *Environ. Sci. Pollut. Res.*, 2023, **30**(3), 7718–7735, DOI: 10.1007/s11356-022-22700-x.

40 I. C. Yadav, N. L. Devi, V. K. Singh, J. Li and G. Zhang, Spatial Distribution, Source Analysis, and Health Risk Assessment of Heavy Metals Contamination in House Dust and Surface Soil from Four Major Cities of Nepal, *Chemosphere*, 2019, **218**, 1100–1113, DOI: 10.1016/j.chemosphere.2018.11.202.

41 Z. Khan, A. Elahi, D. A. Bukhari and A. Rehman, Cadmium Sources, Toxicity, Resistance and Removal by Microorganisms-A Potential Strategy for Cadmium Eradication, *J. Saudi Chem. Soc.*, 2022, **26**(6), 101569, DOI: 10.1016/j.jscs.2022.101569.

42 P. E. Rasmussen, C. Levesque, M. Chénier and H. D. Gardner, Contribution of Metals in Resuspended Dust to Indoor and Personal Inhalation Exposures: Relationships between PM10 and Settled Dust, *Build. Environ.*, 2018, **143**, 513–522, DOI: 10.1016/j.buildenv.2018.07.044.

43 D. P. Franzmeier, G. C. Steinhardt and D. G. Schulze, *Indiana Soil and Landscape Evaluation Manual*, 2004.

44 J. E. Fergusson and D. E. Ryan, The Elemental Composition of Street Dust from Large and Small Urban Areas Related to City Type, Source and Particle Size, *Sci. Total Environ.*, 1984, **34**(1), 101–116, DOI: 10.1016/0048-9697(84)90044-5.

45 R. V. Pouyat, S. D. Day, S. Brown, K. Schwarz, R. E. Shaw, K. Szlavecz, T. L. E. Trammell and I. D. Yesilonis, Urban Soils. in. *Forest and Rangeland Soils of the United States under Changing Conditions: A Comprehensive Science Synthesis*, ed. Pouyat, R. V., Page-Dumroese, D. S., Patel-Weynand, T. and Geiser, L. H., Springer International Publishing, Cham, 2020, pp 127–144, DOI: 10.1007/978-3-030-45216-2_7.

46 M. Crippa, I. El Haddad, J. G. Slowik, P. F. DeCarlo, C. Mohr, M. F. Heringa, R. Chirico, N. Marchand, J. Sciare, U. Baltensperger and A. S. H. Prévôt, Identification of Marine and Continental Aerosol Sources in Paris Using High Resolution Aerosol Mass Spectrometry, *J. Geophys. Res. Atmos.*, 2013, **118**(4), 1950–1963, DOI: 10.1002/jgrd.50151.

47 Y. Chen, D. Q. Rich and P. K. Hopke, Long-Term PM2.5 Source Analyses in New York City from the Perspective of Dispersion Normalized PMF, *Atmos. Environ.*, 2022, **272**, 118949, DOI: 10.1016/j.atmosenv.2022.118949.

48 A. Lambert, A. G. Hallar, M. Garcia, C. Strong, E. Andrews and J. L. Hand, Dust Impacts of Rapid Agricultural Expansion on the Great Plains, *Geophys. Res. Lett.*, 2020, **47**(20), e2020GL090347, DOI: 10.1029/2020GL090347.

49 J. M. Tomlin, K. A. Jankowski, F. A. Rivera-Adorno, M. Fraund, S. China, B. H. Stirm, R. Kaeser, G. S. Eakins, R. C. Moffet, P. B. Shepson and A. Laskin, Chemical Imaging of Fine Mode Atmospheric Particles Collected from a Research Aircraft over Agricultural Fields, *ACS Earth Space Chem.*, 2020, **4**(11), 2171–2184, DOI: 10.1021/acsearthspacechem.0c00172.

50 L. Khachatryan, M. Barekati-Goudarzi, R. Asatryan, A. Ozarowski, D. Boldor, S. M. Lomnicki and S. A. Cormier, Metal-Free Biomass-Derived Environmentally Persistent Free Radicals (Bio-EPFRs) from Lignin Pyrolysis, *ACS Omega*, 2022, **7**(34), 30241–30249, DOI: 10.1021/acsomega.2c03381.

51 K. C. Edwards, S. Kapur, T. Fang, M. Cesler-Maloney, Y. Yang, A. L. Holen, J. Wu, E. S. Robinson, P. F. DeCarlo, K. A. Pratt, R. J. Weber, W. R. Simpson and M. Shiraiwa, Residential Wood Burning and Vehicle Emissions as Major Sources of Environmentally Persistent Free Radicals in Fairbanks, Alaska, *Environ. Sci. Technol.*, 2024, **58**(32), 14293–14305, DOI: 10.1021/acs.est.4c01206.

52 A. Filippi, R. Sheu, T. Berkemeier, U. Pöschl, H. Tong and D. R. Gentner, Environmentally Persistent Free Radicals in Indoor Particulate Matter, Dust, and on Surfaces, *Environ. Sci.: Atmos.*, 2022, **2**, 128–136, DOI: 10.1039/d1ea00075f.

53 A. L. N. Dela Cruz, W. Gehling, S. Lomnicki, R. Cook and B. Dellinger, Detection of Environmentally Persistent Free Radicals at a Superfund Wood Treating Site, *Environ. Sci. Technol.*, 2011, **45**(15), 6356–6365, DOI: 10.1021/es2012947.

54 Y. Wang, S. Li, M. Wang, H. Sun, Z. Mu, L. Zhang, Y. Li and Q. Chen, Source Apportionment of Environmentally Persistent Free Radicals (EPFRs) in PM2.5 over Xi'an, China, *Sci. Total Environ.*, 2019, **689**, 193–202, DOI: 10.1016/j.scitotenv.2019.06.424.

55 X. Guo, N. Zhang, X. Hu, Y. Huang, Z. Ding, Y. Chen and H. Lian, Characteristics and Potential Inhalation Exposure Risks of PM2.5–Bound Environmental Persistent Free Radicals in Nanjing, a Mega–City in China, *Atmos. Environ.*, 2020, **224**, 117355, DOI: 10.1016/j.atmosenv.2020.117355.

56 Q. Chen, M. Wang, H. Sun, X. Wang, Y. Wang, Y. Li, L. Zhang and Z. Mu, Enhanced Health Risks from Exposure to Environmentally Persistent Free Radicals and the Oxidative Stress of PM2.5 from Asian Dust Storms in Erenhot, Zhangbei and Jinan, China, *Environ. Int.*, 2018, **121**, 260–268, DOI: 10.1016/j.envint.2018.09.012.

57 D. Vilcins, P. Dangal, S. Lomnicki, S. A. Cormier, W. R. Lee and P. D. Sly, Household Dust as a Reservoir for Environmentally Persistent Free Radicals: A Longitudinal Study, *Int. J. Environ. Health Res.*, 2026, **36**(1), 122–133, DOI: 10.1080/09603123.2025.2495202.

58 F. He, J. Lu, Z. Li, M. Li, Z. Liu and Y. Tong, Characteristics of Environmentally Persistent Free Radicals in PM2.5 and the Influence of Air Pollutants in Shihezi, Northwestern China, *Toxics*, 2022, **10**(7), 341, DOI: 10.3390/toxics10070341.

59 X. Yang, F. Liu, S. Yang, Y. Yang, Y. Wang, J. Li, M. Zhao, Z. Wang, K. Wang, C. He and H. Tong, Atmospheric Evolution of Environmentally Persistent Free Radicals in

the Rural North China Plain: Effects on Water Solubility and PM$_{2.5}$ Oxidative Potential, *Atmos. Chem. Phys.*, 2024, **24**(19), 11029–11043, DOI: 10.5194/acp-24-11029-2024.

60 H. Li, H. Li, N. Zuo, D. Lang, W. Du, P. Zhang and B. Pan, Can the Concentration of Environmentally Persistent Free Radicals Describe Its Toxicity to *Caenorhabditis Elegans*? Evidence Provided by Neurotoxicity and Oxidative Stress, *J. Hazard. Mater.*, 2024, **469**, 133823, DOI: 10.1016/j.jhazmat.2024.133823.

© 2026 The Author(s). Published by the Royal Society of Chemistry

Environ. Sci.: Adv., 2026, **5**, 866–877 | **877**